Influence of Nozzle-to-Skin Distance in Cryogen Spray Cooling for Dermatologic Laser Surgery

Guillermo Aguilar, PhD,[1,2,*] Boris Majaron, PhD,[2,3] Karl Pope, MS,[4] Lars O. Svaasand, PhD,[2,5] Enrique J. Lavernia, PhD,[6] and J. Stuart Nelson, MD, PhD[1,2]
[1]*Whitaker Center for Biomedical Engineering, University of California, Irvine, California 92697*
[2]*Beckman Laser Institute and Medical Clinic, University of California, Irvine, California 92612*
[3]*Jožef Stefan Institute, Jamova 39, SI-1000 Ljubljana, Slovenia*
[4]*Candela Corporation, 530 Boston Post Rd, Wayland, Massachusetts 01778-1886*
[5]*Norwegian University of Science and Technology, University of Trondheim, Norway*
[6]*Department of Chemical and Biochemical Engineering and Materials Science University of California, Irvine, California 92697*

Background and Objective: Cryogen sprays are used for cooling human skin during various laser treatments. Since characteristics of such sprays have not been completely understood, the optimal atomizing nozzle design and operating conditions for cooling human skin remain to be determined.
Materials and Methods: Two commercial cryogenic spray nozzles are characterized by imaging the sprays and the resulting areas on a substrate, as well as by measurements of the average spray droplet diameters, velocities, temperatures, and heat transfer coefficients at the cryogen-substrate interface; all as a function of distance from the nozzle tip.
Results: Size of spray cones and sprayed areas vary with distance and nozzle. Average droplet diameter and velocity increase with distance in the vicinity of the nozzle, slowly decreasing after a certain maximum is reached. Spray temperature decreases with distance due to the extraction of latent heat of vaporization. At larger distances, temperature increases due to complete evaporation of spray droplets. These three variables combined determine the heat transfer coefficient, which may also initially increase with distance, but eventually decreases as nozzles are moved far from the target.
Conclusion: Sprayed areas and heat extraction efficiencies produced by current commercial nozzles may be significantly modified by varying the distance between the nozzle and the sprayed surface. Lasers Surg. Med. 28:113–120, 2001. © 2001 Wiley-Liss, Inc.

Key words: coalescence; cooling selectivity; cryogen layer; droplet diameter; heat transfer coefficient; momentum; velocity; temperature

INTRODUCTION

Dermatologic laser surgery is the treatment of choice for several dermatoses, *e.g.*, port wine stains (PWS) birthmarks [1,2] and cosmetic treatments, such as hair removal [3] and skin rejuvenation. As has been discussed earlier [4,5,6], the objective of this PWS treatment is to cause selective thermal damage to subsurface targets (chromophores) without causing damage to the overlying epidermis [7].

A solution for *spatially selective cooling of human skin* is to extract heat through the surface rapidly by placing a low-temperature cooling medium adjacent to the skin. This can be achieved by cryogen spray cooling (CSC) [1,8], which consists of a cryogen liquid released from a pressurized container and atomized into a fine spray by a nozzle. Spray droplets evaporate as they move from the nozzle toward the skin surface, extracting in the process the heat of vaporization from the remaining liquid and, therefore, cooling the cryogen below its boiling temperature (T_b) [9,10]. Once cryogen droplets reach the surface, heat is removed from the skin as cryogen continues to evaporate. The only FDA-approved cryogen compound currently used in dermatology is tetrafluoroethane ($C_2H_2F_4$, also known as R-134a), with $T_b = -26°C$ at atmospheric pressure. From earlier studies, it is well known that the spray temperature (T) varies between $-25°C$ to $-60°C$, depending primarily on the distance from the nozzle to the skin surface [9,10,11] and the atomizer nozzle design [10,12,13].

In addition to T, which has a decisive impact on the dynamics of skin cooling, average droplet diameter (D) and velocity (V) may also vary with distance from the nozzle (z). D is expected to decrease with z as cryogen droplets evaporate, and so is V, as drag forces decelerate moving droplets. When z is too short, cryogen ejected from the nozzle may not completely disperse. This results in relatively large, fast-moving droplets, which could splash and bounce off the skin surface without extracting much heat. Furthermore, the total spray volume-to-surface ratio

Contract grant sponsor: Whitaker Foundation; Contract grant number: 482560-59109; Contract grant sponsor: Candela Laser Corporation, NSF; Contract grant number: CTS-9901375.
*Correspondence to: Guillermo Aguilar, PhD, Beckman Laser Institute and Medical Clinic, 1002 Health Sciences Road East, Irvine, CA 92612-1475. E-mail: gaguilar@bli.uci.edu
Accepted 23 October 2000

is not maximized, resulting in less efficient cooling. Alternatively, when z is very long, cryogen droplets may eventually disperse into vapor, resulting in ineffective heat transfer at the skin surface.

The most efficient cooling occurs when the mass flux of sprayed cryogen matches the evaporation rate at the skin surface. Clearly, if not enough cryogen is supplied, optimal heat extraction is not achieved. On the other hand, if the spray mass flux exceeds the evaporation rate, a layer of liquid cryogen may build up on the skin surface, reducing the cooling rate due to rather poor thermal conductivity of liquid cryogen [14]. However, these considerations do not take into account the dynamics of droplet impact and cryogen deposition, which may also affect the cooling efficiency. Our recent studies have demonstrated that 1.4-mm inner diameter straight-tube nozzles produce less atomized sprays with bigger and faster droplets and, thus, lead to increased cooling rates compared to those obtained with sprays of 0.7-mm diameter nozzles, which produce smaller and slower droplets [13].

Another relevant characteristic of CSC is the size of the sprayed area. Ideally, the cryogen spray should cover the entire area exposed to the laser beam. Since the sprayed area varies with z, adjustment of this distance becomes critical in determining the optimal operating conditions.

The present study focuses on determination of the most appropriate positioning of two commercial spray nozzles, based on imaging of spray shapes and sprayed areas, and the dependence on z of the average values of spray droplet diameter (D), velocity (V), temperature (T), and the heat transfer coefficient (h) at the cryogen-substrate interface—which is proportional to the heat extraction rate. The results are discussed in the context of those obtained from recent studies involving nozzles of different diameters [13].

MATERIALS AND METHODS

Spray Forming Setup

Two commercial cryogen spray nozzles used for laser treatment of vascular lesions and hair removal were studied: ScleroPLUS^{TM} (SP), and GentleLASE^{TM} (GL) (both by Candela, Wayland, MA), with approximate inner diameters of 0.8 and 0.5 mm, respectively. Cryogen was delivered through a standard high-pressure hose connecting the cryogen container to the control valve. The R-134a container is pressurized at the saturation pressure of this cryogen (6.7 bar at 25°C). Spurt durations—defined by the time the valve remains open—are electronically controlled. In this study, we have characterized sprays that are longer than 50 milliseconds, so only the characteristics of fully developed sprays are considered [12], i.e., sprays that, on average, do not vary with time.

Imaging Systems

A progressive-scan CCD camera with a shutter speed of 60 microseconds (9700 TMC by Pulnix, Sunnyvale, CA) was used to obtain images of the spray shapes. A flash lamp (FX-1160 by EG & G Electronics, Salem, MA) provides illumination gating by 5 microseconds long pulses, which helps capture flying cryogen droplets. The camera was positioned 900 mm from the nozzle tip, directed perpendicularly to the spray axis. The flash lamp was directed toward the nozzle tip 140 mm away, at a 30° angle with respect to the camera axis. All images were taken under equal lighting conditions. With this arrangement it was possible to obtain a field of view of about 120 mm in length.

To determine the sprayed areas, a high-speed video camera (Encore, Olympus America, Strongsville, OH) was used. The camera was recording at a rate of 1,000 frames per second and a shutter speed of 1/20,000 seconds. A transparent plastic plate was used as the target, and the camera was placed on the opposite side to image the sprayed area. This plate was front and back lit to help illuminate the cryogen and a gray mat was placed around the nozzle to increase the imaging field contrast. The tip of the nozzles was positioned 30, 50, 70, 90, and 120 mm away and perpendicular to the plate.

Ensemble Droplet Size Measurements

An ensemble particle concentration and sizing apparatus (EPCS by Insitec/Malvern, Worcestershire, UK) was used to measure average diameters (D) of the droplets. The operation of this instrument is based on diffraction of a monochromatic light beam (from a 670-nm diode laser) caused by the droplets. If the spray is monodisperse, the diffraction pattern is made of a series of alternate light and dark concentric rings (Fraunhofer diffraction), and spacing between these rings is related to droplet diameter. For polydisperse sprays, a number of these Fraunhofer patterns are superimposed, but the diffraction pattern can still be associated with a droplet diameter distribution [15]. Since the laser beam is perpendicular to the spray axis, the EPCS measurements represent an average over the whole cross section of the spray. To obtain more localized measurements of D, the diameter of the laser beam was reduced from 10 to 3.3 mm with an inverted beam expander (OptoSigma, Santa Ana, CA). A traverse system was used to position the nozzles from 15 to 250 mm perpendicular to the laser beam.

Local Droplet Size and Velocity Measurements

A phase Doppler particle analyzer (PDPA by TSI, St. Paul, MN) was utilized to provide statistical average diameters (D) and velocities (V). PDPA captures and analyzes light scattered by droplets traveling through interfering laser beams of different wavelengths, focused on a probe volume, typically smaller than 1 mm^3. When droplets interfere with these beams, they generate a Doppler signal with a frequency shift proportional to droplet velocity. The phase difference between the signals collected by two adjacent detectors is proportional to droplet diameter. Droplet diameter measurements were carried out with both the EPCS and PDPA apparatus. However, since EPCS represents an ensemble measurement, as opposed to the PDPA, which measures in a small probe volume, it was decided that EPCS measurements better represent the average diameter (D) of the whole spray. In this study, we chose the median diameter (D_{50}) as an average droplet diameter (D).

Temperature Measurements

Spray temperature as a function of distance from the nozzle tip, $T(z)$, was measured with a type-K thermocouple with a bead diameter of approximately 0.3 mm (5SC-TT-E-36 by Omega, Stamford, CT). The estimated response time of this thermocouple is 40 ms in still water at 100°C, and its ASTM standard wire error is ± 2.2°C for the range of temperatures measured. Cryogen spurts of at least 1 second were used to ensure steady state temperature measurements. The temperature sensor was supported by a rigid stick, inserted into the center of the spray cone, and gradually displaced. The estimated uncertainty in z is ± 0.5 mm. Since water condensation and freezing on the thermocouple bead could affect temperature measurements, experiments were conducted in a chamber filled with dry air (relative humidity below 5%). Under such conditions, there was no appreciable condensation or frost formation, except for experiments carried out at $z>100$ mm.

Heat transfer coefficient measurements

A custom-made device was built to measure the heat transfer coefficient (h). In short, the device consists of a silver disk (10.48 mm diameter, 0.42 mm thickness), embedded in a thermal insulator, e.g., epoxy. The upper surface of the disk is exposed to the cryogen spray, and the disk temperature is monitored by a type-K thermocouple attached to its lower surface. The energy equation, which describes the disk temperature evolution is:

$$\rho_{\mathrm{m}}, C_{\mathrm{m}} V_{\mathrm{m}} \frac{\mathrm{d}T}{\mathrm{d}t} = A_{\mathrm{m}} h_{\mathrm{cryo}} (T - T_{\mathrm{cryo}}) \quad (1)$$

where ρ_m, C_m, C_m and A_m are the density, specific heat, volume, and exposed surface area of the metallic disk, respectively, h the heat transfer coefficient, and T and T_{cryo} the temperature of the disk and the cryogen, respectively. This equation assumes that T is uniform over the whole disk at any given time. This assumption means that the disk relaxation time—given by ($\rho_m V_m C_m$)/(A_m h), is much larger than the diffusion time across the disk thickness, d_m^2/α, where d_m is the disk thickness and α its thermal diffusivity. Substituting T_{cryo} with measured spray temperature, h can be calculated from measurements of disk temperature during CSC.

RESULTS

Figure 1 presents photographs of sprays from the two commercial nozzles with different inner diameters: 0.8 mm (SP) and 0.5 mm (GL). Each image was captured at least 60 milliseconds after the beginning of a 300-milliseconds cryogen spurt. Values indicated in Figure 1 are the average cone diameters, D_c, and standard deviations as obtained from nine images acquired at each of the five locations (30, 50, 70, 90 and 120 mm). The values of D_c were estimated as the width of the bright region resulting from the light scattered by the spray droplets. The sprays appear to have cone-like shapes, with D_c initially increasing with z. However, D_c starts decreasing as z approaches 120 mm.

Figures 2 and 3 show the sprayed areas produced by the 0.8 and 0.5-mm diameter nozzles, respectively. Each image was captured 70 milliseconds after the beginning of 100-milliseconds spurts. Images *a* through *e* correspond, respectively, to $z = 30$, 50, 70, 90 and 120 mm. Circles or ellipses drawn in each image mark the approximate effective diameter of the sprayed area (D_s), defined as the continuous bright region produced by the cryogen deposited on the transparent plate.

To illustrate the results more clearly, Figure 4 shows D_s values along with D_c as a function of z. As one would expect, D_s is larger than D_c for both nozzles at all distances. Interestingly, however, whereas the D_s/D_c ratio varies between 1.2 to 3 for the 0.8 mm diameter nozzle, it varies between 2 to 6 for the 0.5 mm diameter nozzle. Furthermore, sprays of the 0.5 mm diameter nozzle have consistently a smaller cone diameter, but their sprayed areas are larger.

Figure 5 shows the average droplet diameter (D), velocity (V), temperature (T) and heat transfer coefficient (h) as a function of z for sprays from the 0.8-mm nozzle. As seen in Figure 5a, the maximum droplet diameter for this nozzle is $D_{max} = 8.7 \pm 0.2$ mm, measured at $z = 60 - 70$ mm. The measurements of V for the same nozzle are presented in Figure 5b. These results show a similar behavior to that of D, with an increasing trend within the first 40 mm from the nozzle. At larger distances, V monotonically decreases, reaching 15 m/seconds at $z = 200$ mm.

Measurements of T are depicted in Figure 5c. An extrapolation of the temperature trend indicates that the exit temperature, T_0, is around -37°C. The minimum temperature, T_{min}, is around -58°C, reached at $z = 60 - 80$ mm, and T starts to increase at $z > 80$ mm.

Finally, Figure 5d shows the variation of h with z. The values shown represent averages over the duration of the spurt (100 milliseconds) as well as over the detector area. After reaching a maximum value of $h_{max} \approx 8{,}400$ W/m^{2}K at $z = 30$ mm, h decreases to about 200 W/m^{2}K at $z = 200$ mm.

Figure 6 presents the same measurements performed with the 0.5-mm nozzle, which shows a qualitatively similar behavior. Figure 6a indicates a somewhat smaller D_{max} reached at a slightly shorter distance. Figure 6b shows an increase in V (for z<30 mm), which is less pronounced than for the 0.8-mm nozzle. V_{max} is also smaller, and is reached at a slightly shorter distance. Figure 6c shows the variation of T with z. Note that while T_0 is 11°C lower for the 0.5 mm nozzle, T_{min} is the same for both nozzles. Finally, Figure 6d shows the variation of h with z. The maximum value, h_{max}, is about 6,200 W/m^{2}K and is reached at $z = 50$ mm, and h decreases from 6,000 to 200 W/m^{2}K between $z = 20$ and 120 mm.

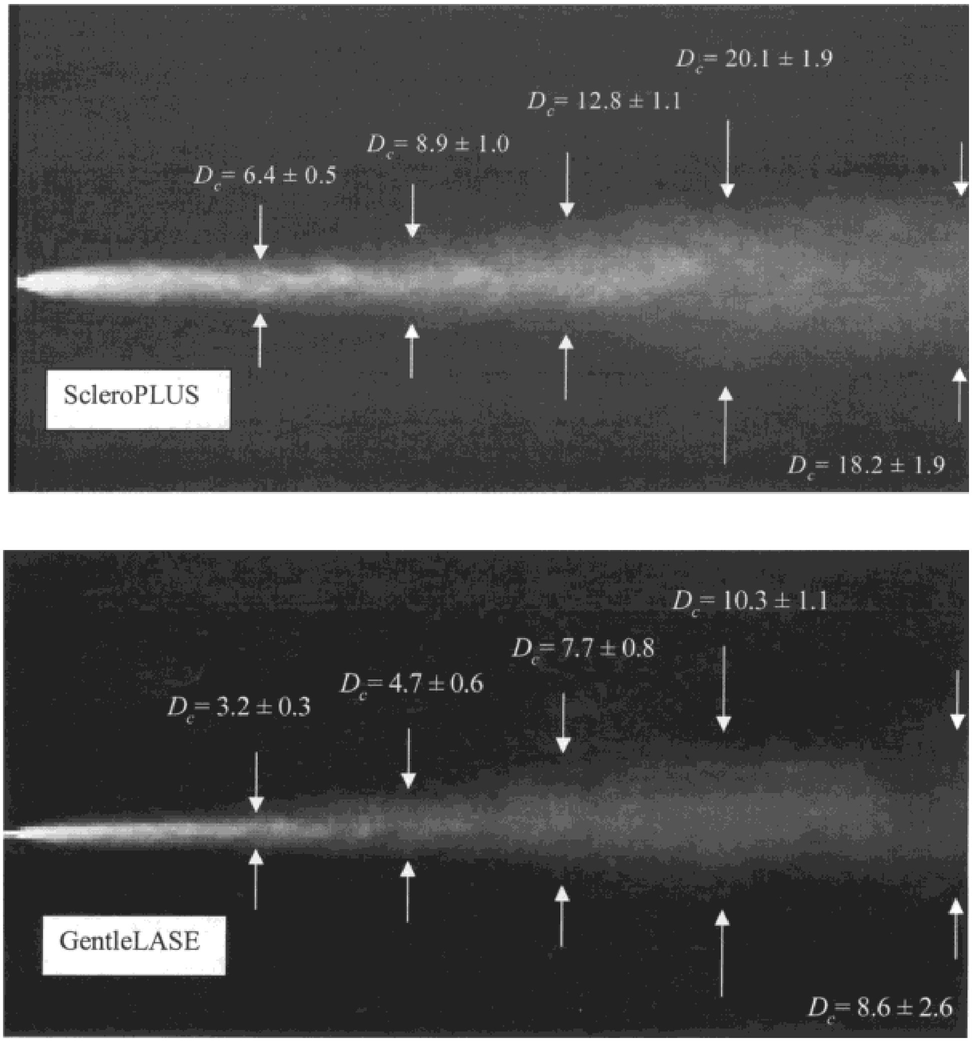

Fig. 1. Photographs of cryogen sprays ejected by the 0.8 (SP) and 0.5-mm (GL) nozzles, respectively. At the locations indicated by the arrows ($z = 30$, 50, 70, 90, and 120 mm), the average spray cone diameter (D_c) and standard deviation are indicated.

Table 1 summarizes the relevant extreme values of the measured variables, and the ranges of z where they occur.

DISCUSSION

As could be expected, Figures 1 through 4 indicate that D_c and D_s initially increase with z for both nozzles. The reduction in D_c at larger distances can be attributed to complete evaporation of smaller droplets [16], which evaporate before the larger ones. The 0.5-mm nozzle produces a smaller cone diameter (D_c) than the 0.8-mm nozzle, and yet a larger sprayed area (D_s). This difference between nozzles indicates that, whereas for the 0.8-mm diameter nozzle spray droplets expand over a larger area before impinging onto the skin, a certain amount of droplets bounce back and disperse as small clusters of liquid cryogen surrounding the central area—as suggested by Figure 2 (especially Figs. 2a and 2b). In contrast, spray droplets from the 0.5-mm diameter nozzle do not bounce back as much, which suggests that they have smaller momentum, adhere better to the sprayed surface and, thus, generate a wider and more homogeneous layer at the same z.

The droplet diameter growth seen in Figure 5a for $0 < z < 60$ mm, is an indication of droplet coalescence [17,18], a phenomenon that may contribute more to the average droplet diameter variation than the evaporation process. However, evaporation becomes the dominant process in determining the average droplet size for $z > 60$ mm, as demonstrated by decreasing D at larger z.

The increase of V within the first 40 mm (Fig. 5b), can be explained by the coalescence of large fast droplets, with slower smaller ones. The decrease of V for $z > 40$ mm results from droplet deceleration due to drag as droplets move through quiescent air [10,12].

For the 0.5 mm nozzle, T_{min} and D_{max} are reached at $z \sim 60$–80 mm, V_{max} is reached at $z = 40$ mm, whereas h is

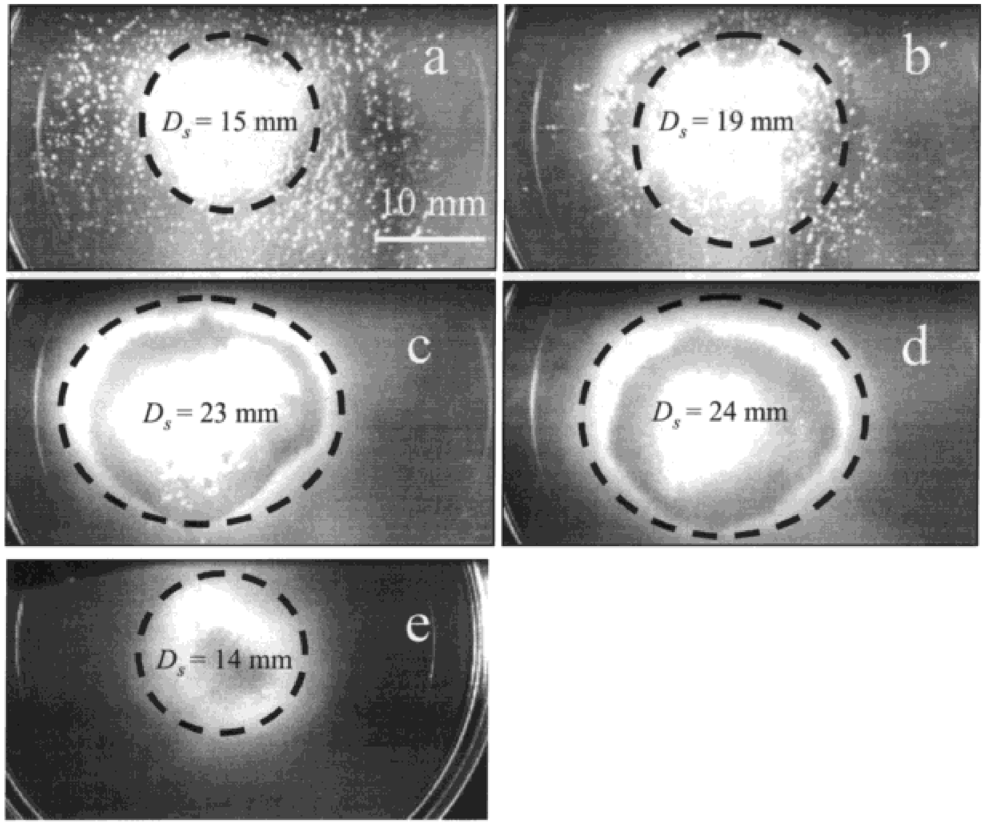

Fig. 2. Photographs of cryogen spray areas produced by the 0.8-mm nozzle. Images **a–e** correspond to nozzle tip-to-target distances (z) of 30, 50, 70, 90, and 120 mm, respectively. Each photograph was taken 50 milliseconds after the beginning of a 70-ms spurt. Effective sprayed area diameters (D_s) are indicated on each image.

maximal at $z = 30$ mm (see Table 1). Clearly, the complexity of the problem is such that establishing a correlation between D, V, T, and h, is not straightforward. Nevertheless, it is noted that a relatively invariant value of h is reached between 40 and 70 mm, the same range where D is maximum. This is perhaps an indication that the influence of D on h may actually be more dominant than that of V.

This study shows that large variations of h can be achieved by positioning the nozzles at different distances.

For laser therapy of PWS or other superficial targets, it is important that the effect of cooling remains spatially confined to the superficial 100–200 μm of the skin [1,8]. Such spatial selectivity requires the use of short cryogen spurts (tens to hundreds of milliseconds) and the highest possible heat transfer rates. Therefore, aiming at the highest h that this nozzle can produce ($h_{max} = 8{,}400$ W/m^{2}K) should be the most important criterion to determine its appropriate position with respect to the skin surface. If z is adjusted between 15 and 30 mm, h remains relatively constant around its maximum value. One should be aware, however, that the second most important criterion for the optimal use of CSC is the precise control over D_s. If the goal was to maximize D_s only, a range of $z = 90–100$ mm would be the optimal for this nozzle, at the expense of a 36% decrease in h. However, a compromise between both criteria can be met if z is adjusted between 15 and 70 mm, where h varies only by 20%.

Note that the measured values of h may be underestimated as much as 10% due to the heat losses to the insulating material surrounding the metallic disk. In addition, the value of h may vary with experimental conditions such as ambient humidity [19], cryogen container pressure, and possible impurities in cryogen. The qualitative determination of h under similar experimental conditions has been lately a controversial issue with reported values of h between 2,400 [2] and 40,000 W/m^{2}K [13] obtained with different atomizers [10,12], spraying distances, and measurement methods [2,13].

The behavior of the 0.5-mm nozzle sprays is qualitatively very similar to that of the 0.8-mm nozzle sprays (Fig. 6). In particular, D_{max} of the 0.5-mm nozzle is slightly smaller and it is reached at shorter z (see Table 1); V_{max} is somewhat smaller, and is reached at a shorter distance, and the decrease of V seems more rapid thereafter as compared to the 0.8-mm nozzle (see Table 1). These

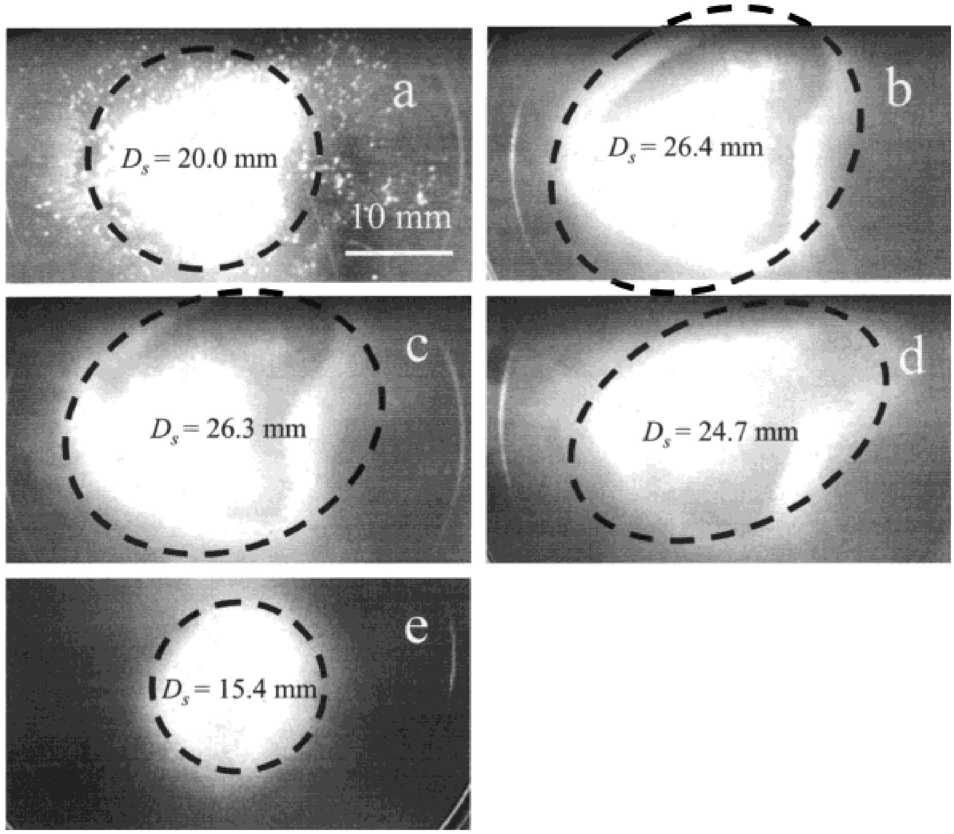

Fig. 3. Photographs of cryogen spray areas produced by the 0.5-mm nozzle. Images **a–e** correspond to nozzle tip-to-target distances (*z*) of 30, 50, 70, 90, and 120 mm, respectively. Each photograph was taken 50 milliseconds after the beginning of a 70-ms spurt. Effective sprayed area diameters (D_s) are indicated on each image.

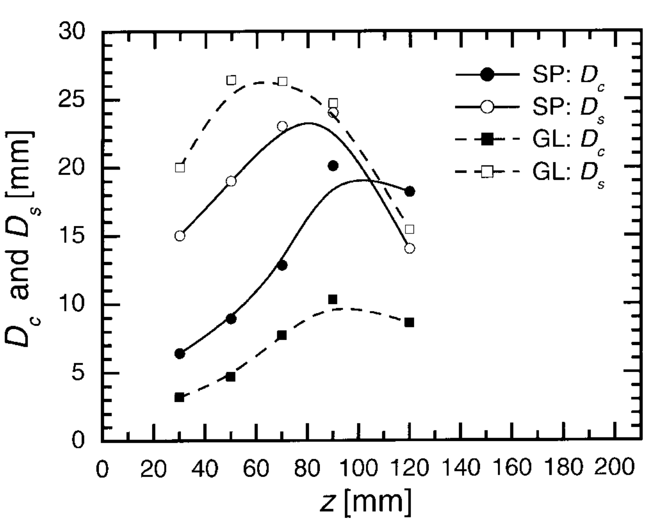

Fig. 4. Average cone diameter (D_c) and effective sprayed area diameter (D_s) as a function of distance from the nozzle (*z*) produced by the 0.8 and 0.5-mm nozzles, respectively. Values extracted from measurements reported in Fig. 1–3.

quantitative differences in $D(z)$ and $V(z)$ between the two nozzles result in different behavior of h. For the 0.5 mm nozzle, h_{max} is 6,200 W/m^{2}K, and is reached approximately at $z = 50$. In this case too, a dominant influence of D is indicated, since h_{max} occurs within the same range as D_{max}.

Maximizing h may not be the ultimate goal for CSC aimed at the therapy of deeper targets (e.g., hair removal). In fact, the 0.5-mm nozzle (GL) is currently used with an Alexandrite laser for the treatment of deep targets and for such targets, it may actually be beneficial to reduce h in order to have a more prolonged and less aggressive heat extraction, while still obtaining sufficient epidermal protection [19,20].

From Figures 4 and 6 one can appreciate that it is possible to control D_s by varying z between 15 and 50 mm with only a 16% variation in h. By increasing the distance beyond $z = 50$ mm, it is possible to reduce h to basically any desired value. Finally, if values of h between 6,000 and 3,000 W/m^{2}K are permissible, D_s can be maximized if the 0.5-mm nozzle is positioned within the range of $z =$ 50–70 mm.

Another way of controlling h is by varying the nozzle diameter. Previous studies have shown that nozzles with larger diameters can effectively augment heat extraction

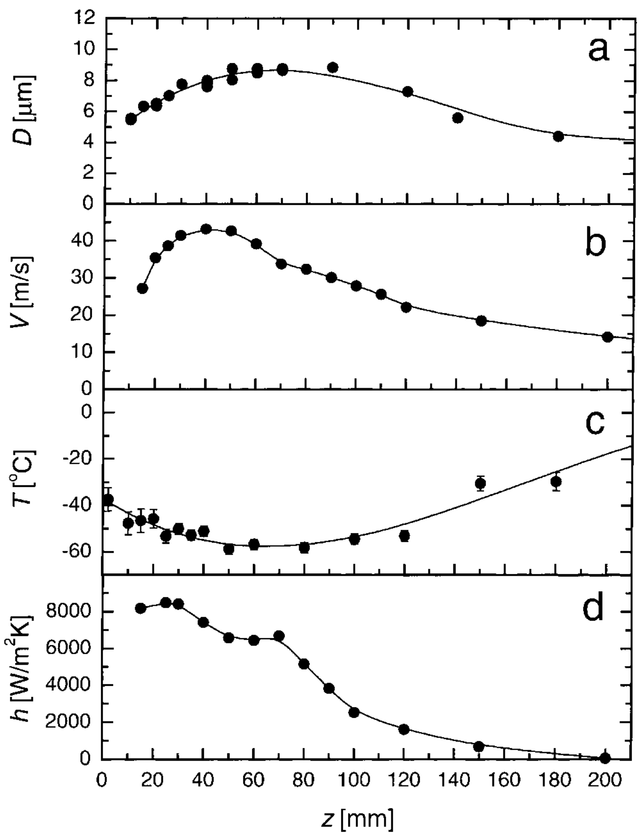

Fig. 5. Average droplet diameter (D), velocity (V), temperature (T) and heat transfer coefficient (h), measured as a function of distance from the nozzle tip (z) for the 0.8-mm nozzle.

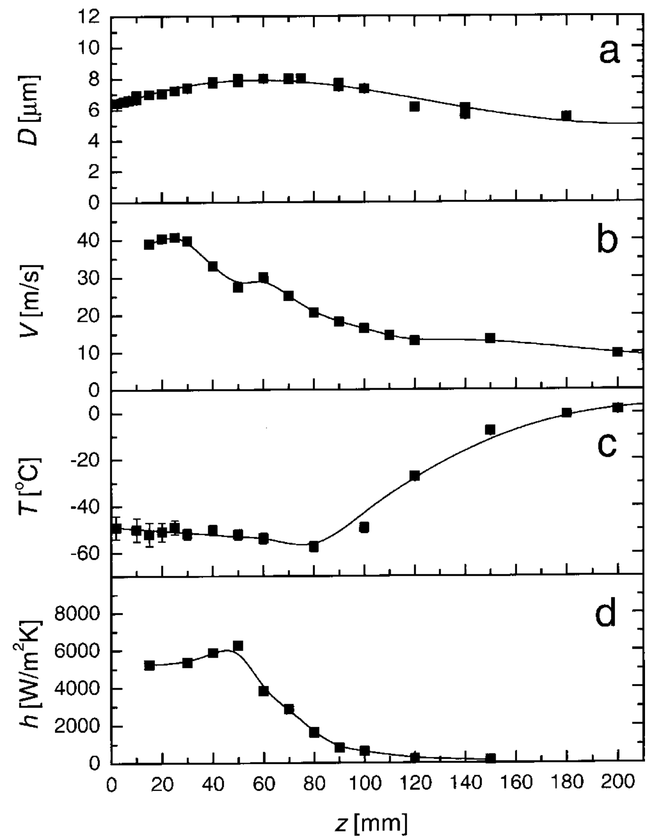

Fig. 6. Average droplet diameter (D), velocity (V), temperature (T) and heat transfer coefficient (h), measured as a function of distance from the nozzle tip (z) for the 0.5-mm nozzle.

from skin [13], suggesting that droplet momentum is important for maximization of h. This study confirms that the larger diameter nozzle (SP) produces higher momentum sprays which, for the most part, result in higher h. Note also that T starts to increase at about $z = 100$–120 mm for the 0.8-mm nozzle (SP), while for the 0.5 mm one (GL), this increase is noticeable at about 80 mm. This is consistent with D and V measurements, since the higher momentum droplets (those of 5P) move farther downstream before evaporating completely.

TABLE 1. Relevant Extreme Values of Cone Diameter (D_c), Sprayed Area Diameter (D_s), D_s/D_c Ratio, Average Droplet Diameter (D), Velocity (V), Temperature (T), Initial Temperature (T_0) and Heat Transfer Coefficient (h) Measured for 0.8 and 0.5-mm Nozzle Sprays

	ScleroPLUS (inner diameter = 0.8 mm)		GemtleLASE (inner diameter = 0.5 mm)	
Variable	Value	z [mm]	Value	z [mm]
$D_{c,max}$ (mm)	20	90	10	90
$D_{s,max}$ (mm)	23	90–100	26	50
D_s/D_c	1.2-3	—	2–6	—
D_{max} (μm)	8.7	60–70	8	50–60
V_{max} (m/s)	45	40	42	30
T_{min} (°C)	− 58	60–80	− 58	60–80
T_0 (°C)	− 37	0	− 48	0
h_{max} (W/m^2 K)	8,400	30	6,200	50

Unfortunately, the use of larger diameter nozzles may not be viable for clinical applications, since they produce more confined jet-like sprays, and larger droplet momentum may produce patient discomfort. In contrast, smaller diameter nozzles produce a finely atomized spray, which is more gentle to patients and cover a wider sprayed area. However, the downside of fine atomization is that it may induce the formation of a thicker liquid layer, which adversely affects the heat extraction rate due to the low thermal conductivity of cryogen [13,14].

We are currently experimenting with a proportional valve, which enables control of the sprayed area at a fixed spraying distance.

CONCLUSIONS

1. The 0.5-mm nozzle (GL) sprays show smaller spray-cone sizes but larger sprayed areas than the 0.8-mm nozzle (SP) sprays. These results suggest that the 0.5-mm nozzle produces cryogen spray that adheres better to the sprayed surface, generating a wider and more homogeneous layer on the skin at the same distance from the nozzle (z). Maxima of D_s for the 0.8 and 0.5-mm nozzles are achieved at $z = 90-100$ and $50-70$ mm, respectively.
2. Measurements of h show a maximum value of 8,400 W/m^2K at about $z = 30$ mm for the 0.8-mm nozzle. In order to vary D_s, z may be adjusted between 15 to 30 mm without significantly affecting h (<20%).
3. The 0.5-mm nozzle shows $h_{max} = 6{,}200$ W/m^2K at about $z = 50$ mm. For the application of this nozzle, a reduction of h and maximization of D_s may actually be desirable. This can be achieved by increasing z beyond 50 mm.
4. For each nozzle, relatively invariant values of h are reached close to the ranges of z where D is maximal, suggesting that the influence of droplets mass (D) may actually be the most determinant variable on the value of h.

ACKNOWLEDGMENTS

The authors wish to acknowledge the financial support from the Whitaker Foundation; equipment donation and grant (482560-59109 to EJL and JSN) from Candela Laser Corporation; NSF grant (CTS-9901375 to EJL) for the purchase of the PDPA system; the support from the Institute of Arthritis and Musculoskeletal and Skin Diseases; research grant awarded at the National Institutes of Health to JSN (AR43419); the Institutional support from the Department of Energy, Office of Naval Research, National Institutes of Health and the Beckman Laser Institute and Medical Clinic Endowment. BM was supported in part by the Slovenian Ministry of Science and Technology. The laboratory assistance provided by Emil Karapetian, Yung-Hsiang Judy Hsu and Brooke Basinger and helpful discussions with Sol Kimel are also appreciated.

REFERENCES

1. Nelson JS, Milner TE, Anvari B, Tanenbaum BS, Kimel S, Svaasand LO, Jacques SL. Dynamic epidermal cooling during pulsed laser treatment of port-wine stain. Arch Dermatol 1995;131:695–700.
2. Torres JH, Nelson JS, Tanenbaum BS, Milner TE, Goodman DM, Anvari B. Estimation of internal skin temperature measurements in response to cryogen spray cooling: implications for laser therapy of port wine stains. IEEE J Special Topics Quant Elect 1999;5:1058–1066.
3. Altshuler GB, Zenzie HH, Erofeev AV, Smirnov MZ, Anderson RR, Dierickx C. Contact cooling of the skin. Phys Med Biol 1999; 44:1003–1023.
4. Milner TE, Goodman DM, Tanenbaum BS, Nelson JS. Depth profiling of laser heated chromophores in biological tissues using pulsed photothermal radiometry. J Optical Soc Am A 1995; 12:1479–1488.
5. Nelson JS, Milner TE, Tanenbaum BS, Goodman DM. Space dependent temperature increase in human skin subsurface chromophores immediately following pulsed laser exposure. Proc SPIE 1996; 2623:20–31.
6. Milner TE, Goodman DM, Tanenbaum BS, Anvari B, Svaasand LO, Nelson JS. Imaging laser heated subsurface chromophores in biological materials: determination of lateral physical dimensions. Phys Med Biol 1996; 41:31–44.
7. Chang CJ and Nelson JS. Cryogen spray cooling and higher fluence pulsed dye laser treatment improve port wine stain clearance while minimizing epidermal damage. Dermatol Surg 1999; 25:766–771.
8. Nelson JS, Milner TE, Anvari B, Tanenbaum BS, Svaasand LO, Kimel S. Dynamic epidermal cooling in conjunction with laser-induced photothermolysis of port wine stain blood vessels. Lasers Surg Med 1996; 19:224–229.
9. Aguilar G, Verkruysse W, Majaron B, Zhou Y, Nelson JS, Lavernia EJ. Modeling of cryogenic spray temperature and evaporation rate based on single-droplet analysis. Proc 8th International Conference on Liquid Atomization and Spray Systems; 2000. p. 37–48.
10. Aguilar G, Verkruysse W, Majaron B, Zhou Y, Nelson JS, Lavernia EJ. Theoretical and experimental determination of droplet diameter, temperature, and evaporation rate evolution in cryogenic sprays. Int J Heat Mass Tran 2001 (in press).
11. Anvari B, Ver Steeg BJ, Milner TE, Tanenbaum BS, Klein TJ, Gerstner E, Kimel S, Nelson JS. Cryogen spray cooling of human skin: effects of ambient humidity level, spraying distance, and cryogen boiling point. Proc SPIE 1997; 3192:106–110.
12. Aguilar G, Majaron B, Verkruysse W, Zhou Y, Nelson JS, Lavernia EJ. Characterization of cryogenic spray nozzles with application to skin cooling, Proc. International Mechanical Engineering Congress and Exposition (IMECE), ASME 2000; FED-V. 253:189–197.
13. Verkruysse W, Majaron B, Aguilar G, Svaasand LO, Nelson JS. Dynamics of cryogen deposition relative to heat extraction rate during cryogen spray cooling. Proc SPIE 2000; 3907: 37–58.
14. Estes, KA, Mudawar, I. Correlation of Sauter mean diameter and critical heat flux for spray cooling of small surfaces. Int. J. Heat Mass Transfer 1995;38:2985–2996.
15. Lefevbre AH. Atomization and Sprays, 1st edn. New York. Taylor & Francis. 1989: p 309.
16. Bayvel L and Orzechowski Z. Liquid Atomization. In: Norman Chigier, editor. Washington DC: Taylor and Francis. 1993. p 131–143.
17. Orme M, Experiments on droplet collisions, bounce, coalescence and disruption. Prog. Energy Combustion Sci 1997; 23: 65–79.
18. Nishitani R, Kasuya A, Nishina Y. In situ STM observation of coalescence of metal particles in liquid, Zeitschrift fur Physik D 1993; 26:S42–S44.
19. Majaron B, Kimel S, Verkruysse W, Aguilar G, Pope K, Svaasand LO, Lavernia EJ, Nelson JS. Cryogen spray cooling in laser dermatology: effects of ambient humidity and frost formation; Lasers Surg Med (submitted).
20. Nelson JS, Majaron B, Kelly KM. Active skin cooling in conjunction with laser dermatologic surgery: Methodology and clinical results; Seminars Cutaneous Med Surg 2000;19:253–266.